

# Nonlinear Contact Analysis of Gear Teeth for Malfunction Diagnostics

*D. Kong<sup>1</sup>, J.M. Meagher<sup>2</sup>, C. Xu<sup>1</sup>, X. Wu<sup>2</sup> Y. Wu<sup>1</sup>*

<sup>1</sup>College of Mechanical Science and Engineering, Jilin University, Changchun 130025, P.R. China

<sup>2</sup>Department of Mechanical Engineering, California Polytechnic State University, San Luis Obispo, CA. 93407

[xwu@calpoly.edu](mailto:xwu@calpoly.edu)

## NOMENCLATURE

d	Penetration depth
$d_1$	Diameter of standard pitch circle
e	Contact Force exponent
i	Gear Ratio, gear/ pinion
$x_0$	Initial size of the deformable body
x	Distance between the contacting bodies
C	Damping coefficient
$E_1, E_2$	Young's Modulus of pinion and gear respectively
$E^*$	Equivalent Young's Modulus of two contacting bodies
F	Contact force
K	Stiffness
R	Equivalent radius of two contacting bodies
S	Step function
$\alpha_t', \alpha_t$	Transverse pressure angle at engaged, standard pitch circle
$\beta, \beta_b$	Helical angle at the pitch, base circle
$\nu_1, \nu_2$	Poisson ratio of the pinion and gear respectively

## ABSTRACT

Gearboxes sustain a variety of faults such as broken-shafts, eroded, broken, or missing teeth, and even broken-cases. Casing mounted accelerometers can detect fault patterns but the signals are complicated and difficult to interpret. This study considers the tooth loading of ideal gears and gears with defects. A large industrial gearbox used in a 12m<sup>3</sup> electric mining shovel is modeled. The nonlinear contact mechanics is analyzed to predict the bearing supporting force variation vs. the gear tooth loading after a 3-D CAD model of the gearbox is transferred into multi-body dynamics software. The contact mechanics model of the meshing teeth is built by careful calculation and selection of the contact simulation parameters such as the stiffness, force exponent, and damping and friction coefficients. To simulate the real working environment of the gearbox, simulated bearing support forces are mixed with white noise. The signal is subsequently processed by the Db5 wavelet of the MATLAB Wavelet toolbox. Wavelet analysis results show that bearing supporting force fluctuation cycle is almost the same with that of the meshing forces of the fault gearing pairs, which could be used to predict the tooth malfunction of the gearbox.

Keywords: Malfunction Diagnostics, Contact Mechanics, Gearbox, Wavelet, Simulation

## 1. Introduction

Gearboxes of construction vehicles like electric mining shovels and dump trucks sustain a variety of faults such as broken-shafts, eroded, broken, or missing teeth, and even broken-cases because of heavy loads and harsh working conditions. Early malfunction detection is important to limit damage and avoid accidents. Generally, casing mounted accelerometers are used to detect gearbox faults based on vibration analysis techniques. Frequency/cepstrum analysis, time/statistical analysis, and time-frequency analysis have all been used by many researchers. Wang *et al.* [1] experimentally tested healthy, cracked, spalled, and chipped gear teeth and compared the sensitivity and robustness of the different data processing techniques. Dalpiaz *et al.* [2] investigated a gear pair with a fatigue crack and discussed the effectiveness and sensitivity of the time-synchronous average (TSA) analysis, cyclostationary analysis, and traditional cepstrum analysis on the basis of experiment. Parey *et al.* [3] developed a six DOF nonlinear model for a pair of spur gears on 2 shafts, calculated the Hertzian stiffness for the tooth surface contact, and implemented the empirical mode decomposition (EMD) method to simulate the different defect widths. Different methods of estimating stiffness have been utilized by a number of authors [4-9]. Previous research shows that the fault signal patterns are very complicated and depend on specific gear pairs, i.e., the signals from a specific gearbox are difficult to interpret until a series of modeling, testing and data processing work are carried out. However, it is not practical to test each type of gearbox, especially a large one, for the specific fault patterns. To solve this issue, a virtual experiment method based on multi-body dynamics and nonlinear contact mechanics simulation is presented.

The crawler traveling gearbox of a 12 m<sup>3</sup> electric mining shovel is investigated in this paper to predict the bearing supporting force variation vs. the gear tooth loading based on the nonlinear contact mechanics analysis. The gearbox is a three-stage, dual-motor driven and dual-output. The drive train of the gearbox is shown in Fig.1 and the technical specifications are listed in Table 1. The 3-D CAD model of the gearbox, as shown in Fig.2, is built by the Pro/Engineer Wildfire software and then transferred into the multi-body dynamics model by the software MSC ADAMS. The driving torques from both of the traveling motors and resistant torques from the crawler system are applied to the input and output shafts of the gearbox respectively. The contact forces of the meshing teeth in the gear set is described by a contact mechanics model which is determined by parameters such as the stiffness, force exponent, and damping and friction coefficients.

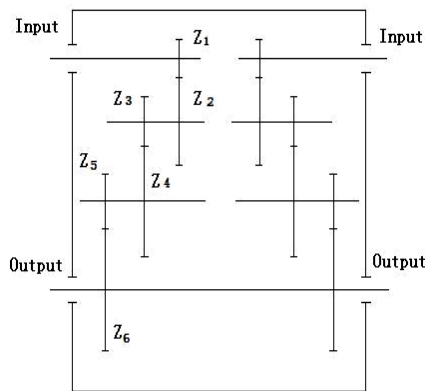


Figure 1: Layout of the Crawler Traveling Gearbox

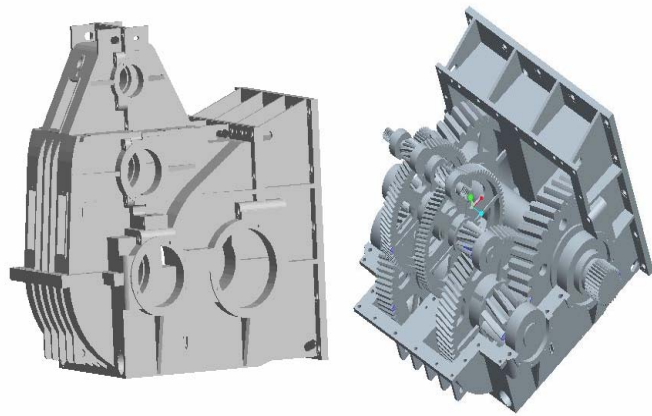


Figure 2: CAD Model of the Gearbox

## 2. Multi-body Dynamics Model

Although the finite element method is a general numerical method applicable to model gear contact with high simulation accuracy, a huge computational effort is required for contact of several pairs of gear wheels in a large gearbox. Rigid body modeling has high computational efficiency, but it can not describe the contact of the meshing gear teeth. Fortunately, commercial multi-body dynamics simulation software MSC ADAMS has the capability of rigid-elastic model computation, which is suitable for the multi-body model of the gearbox. The rigid-elastic model is a compromise between the rigid body and elastic body, in which the shafts and wheel bodies are taken as rigid, but the contact surfaces of the meshing gears are deformable bodies.

**Table 1: Gearbox Technical Specification**

Gear ID	Tooth Number	Normal Modulus	Speed Ratio	Helical Angle	Wheel Center Distance	Gear Widths	Pressure Angle
Z1	11	12mm	7.3636	16°	580mm	130mm	20°
Z2	81					120mm	
Z3	12	16mm	5.666	12°	665mm	210mm	
Z4	68					200mm	
Z5	11	30mm	3.273	12°	750mm	280mm	
Z6	36					270mm	
Total Speed Ratio			i	136.56			
Rated Motor Power			kW	110×2			
Rated Motor Velocity			rpm	740			
Motor Overload Capacity				2.5			
Max. Output Torque of the Gearbox			kNm	437×2=874			

### 2.1 Transformation of the Gearbox Model

The 3-D CAD model of the gearbox, as shown in Fig.2, is transferred into an ADAMS multi-body model using the Mechanical/Pro interface embedded in Pro/Engineer. The case and bearings are hidden for good visual effect of the simulation. The multi-body model of the gearbox is shown in Fig. 3. The bearings to support the wheel shafts in the gearbox are described by revolute and cylindrical joints. A fixed joint is added to every gear wheel and corresponding shaft, so that the torque applied to the input shafts is transferred onto the output shaft. The transferred model should be checked for the consistency with the Pro/Engineer model on mass and density to assure correct transformation.

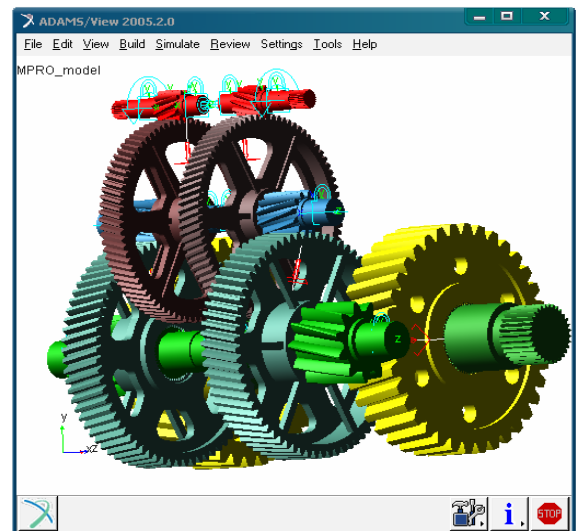


**Figure 3: Multi-body Model of the Gearbox**

## 2.2 Determination of the Contact Parameters

### 2.2.1 The Definition of Contact in ADAMS

The contact force model is shown in Fig. 4. The contact force in ADAMS [12] can be expressed as

$$F = \begin{cases} K(x_0 - x)^e + CS\dot{x} & x < x_0 \\ 0 & x \geq x_0 \end{cases} \quad (1)$$

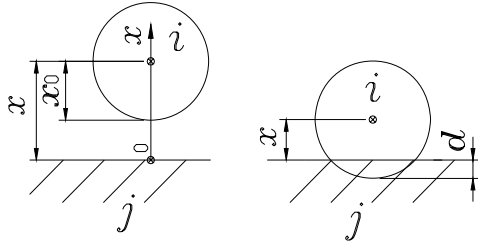


Figure 4: Contact Force Model in ADAMS

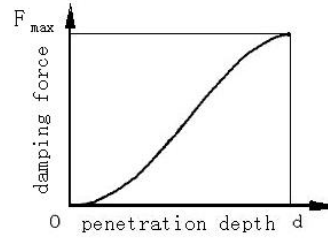


Figure 5: Damping Force vs. Penetration Depth

In Eq.(1),  $x_0 - x$  is the deformation in the process of contact-collision. Eq.(1) shows that the contact does not occur while  $x \geq x_0$  and the contact force is zero. Contact occurs while  $x < x_0$  and the contact force is related to the parameters such as stiffness  $K$ , the deformation  $x_0 - x$ , contact force exponent  $e$ , damping coefficient  $C$  and the penetration depth  $d$  which is the maximum value of  $x_0 - x$ .  $S$  is a step function defined as

$$S = \begin{cases} 0 & x > x_0 \\ (3 - 2\Delta d)\Delta d^2 & x_0 - d < x < x_0 \\ 1 & x \leq x_0 - d \end{cases} \quad (2)$$

In Eq. (2),  $\Delta d = x_0 - x$ , is the deformation of the body. Eq. (1) also shows that the contact force defined in ADAMS is composed of two parts. An elastic component  $K(x_0 - x)^e$ , acts like a nonlinear spring. The other is the damping force  $CS(dx/dt)$ , which is a function of the contact-collision velocity. By the definition of the step function in Eq.(2) we know that the damping force is defined as a cubic function of penetration depth. To avoid the function discontinuity caused by the dramatic variation of the damping force while contact-collision occurs, as shown in figure 5, the damping force is set to zero when the penetration depth of the two contacted bodies is zero, and approaches a maximum value  $F_{max}$  when the specified penetration depth  $d$  is reached.

#### 2.2.2 The Types of Contact

Two types of contact are modeled between the surfaces of the contacted bodies. One type is discontinuous contact, such as a falling ball bouncing on the floor. The other is continuous contact, where the contact is defined as a nonlinear spring. Two algorithms for the computation of contact force are available in ADAMS/View, the Restitution Method and the Impact Method. Considering the computing efficiency and accuracy, the latter is adopted in this paper. Necessary parameters for this method are listed in Table 2. The contact force computed by this method is composed of two parts, the elastic force caused by the deforming components and the damping force caused by the relative deforming velocity.

Table 2: Contact Model Parameters

Stiffness (K)	Static Friction Coefficient ( $\mu_s$ )
Force Exponent( e)	Static Friction Slip Velocity( $v_s$ )
Damping(c)	Dynamic Friction Coefficient( $\mu_d$ )
Penetration Depth( d)	Dynamic Friction Slip Velocity( $v_d$ )

### 2.2.3 Determination of the Parameters for a Helical Gearing Pair Contact Model

(1) Stiffness  $K$ : According to the Hertzian elastic contact theory [10], the stiffness of the two contacted bodies could be described by a pair of ideal contacted cylindrical bodies, and Bi *et al* [8] derived the equivalent radii of the engaged helical gear pair. Consequently, the stiffness could be expressed as

$$\left\{ \begin{array}{l} K = \frac{4}{3} R^{\frac{1}{2}} E^* = \frac{4}{3} \left[ \frac{id_1 \cos \alpha_t \tan \alpha_t'}{2(1+i) \cos \beta_b} \right]^{\frac{1}{2}} E^* \\ \frac{1}{E^*} = \frac{1-\nu_1^2}{E_1} + \frac{1-\nu_2^2}{E_2} \\ \beta_b = a \tan(\tan \beta \cos \alpha_t) \end{array} \right. \quad (3)$$

The materials for the pinions and gears of the gearbox are alloy steel and cast steel respectively, and the values for the Poisson ratio and the Young's Modulus are listed in Table 3. Through calculation, the stiffness values for the three gear pairs in the drive line of the gearbox are listed in Table 4.

Table 3: Gear Material Properties

Item	Gear ID	Material	Young's Modulus	Poisson Ratio
Pinion	Z1,Z3,Z5	Alloy Steel	$2.1 \times 10^5$ N/mm <sup>2</sup>	0.29
Gear	Z2,Z4,Z6	Cast Steel	$1.75 \times 10^5$ N/mm <sup>2</sup>	

Table 4: Stiffness for the Gear Pairs

Gear Pair	Stiffness
Z <sub>1</sub> , Z <sub>2</sub>	$K_1 = 6.824 \times 10^5$ N/mm <sup>3/2</sup>
Z <sub>3</sub> , Z <sub>4</sub>	$K_2 = 8.102 \times 10^5$ N/mm <sup>3/2</sup>
Z <sub>5</sub> , Z <sub>6</sub>	$K_3 = 10.941 \times 10^5$ N/mm <sup>3/2</sup>

(2) Force Exponent  $e$ : Considering numerical convergence and computation speed, a force exponent of  $e=1.5$  is determined by several times of trial simulation.

(3) Damping Coefficient  $C$ : Based on previous experience for gearboxes of this size the damping coefficient generally takes values 0.1%~1% of the stiffness  $K$ . For this study the damping coefficient is set to  $C=1000$  Ns/mm.

(4) Penetration Depth  $d$ : The relationship between damping force and penetration depth is shown in Fig.5. In common cases, a reasonable value for penetration depth is 0.01 mm. We used  $d = 0.1$  here considering the numerical convergence in ADAMS.

(5) Dynamic and Static Friction Coefficient and Viscous Velocity: The materials for the engaged pinions and gears are alloy steel and cast steel respectively, and the meshing pairs are lubricated. The static friction coefficient  $\mu_s$ , static transition velocity  $v_s$ , dynamic friction coefficient  $\mu_d$  and friction transition velocity  $v_d$  listed in Table 5 are typical values found in mechanical design handbooks.

Table 5: Friction Coefficient Values

Static Friction Coefficient( $\mu_s$ )	0.1
Static Transition Velocity( $v_s$ )	1 mm/s
Dynamic Friction Coefficient( $\mu_d$ )	0.08
Friction Transition Velocity( $v_d$ )	10mm/s

### **3. The Algorithm Selection for Nonlinear Contact Dynamics Simulation**

ADAMS offers four stiff stable solvers, the Gstiff, Wstiff, Dstiff and Constant-BDF, to solve the Differential-Algebra Equation (DAE) for the multi-body dynamics simulation. All four solvers use multi-step, variable order algorithms. There are three integration formats, the Index3, SI2 and SI1, available for the DAE solution.

#### **3.1 Comparison of the Integration Formats**

The Index3 (short for I3) format monitors only the error of the displacement and other state variables of the differential equations, but not the velocities and constrained reaction forces. Therefore, the accuracy for computation of the velocity, acceleration and constrained reaction forces is not as good as other formats. The SI2 format is able to control the errors of the Lagrange multiplier and velocity by considering the velocity constrained equations. Therefore, more accurate solutions could be obtained for the velocity and acceleration computation.

The SI1 format is able to monitor all state variables such as displacement, velocity and Lagrange multiplier by introducing the velocity constrained equations, instead of acceleration constrained equations. Therefore, this format has higher accuracy than SI2 format. However, it is too sensitive to the models with friction and contact problems.

#### **3.2 Comparison of the Solvers**

The Gstiff solver is a stiff stable algorithm with characteristics of multi-step, variable order, variable step and fixed coefficients. It could solve the DAE explicitly with I3, SI2 and SI1 formats. The Gstiff solver has the features of fast computation and high displacement accuracy. However, this solver could produce larger error on the computation of velocity. This can produce discontinuities in acceleration. Nevertheless, the error could be controlled by limitation of the maximum step during the simulation.

The Wstiff solver is a stiff stable algorithm with characteristics of multi-step, variable order, variable step and variable coefficients. It could also solve the DAE explicitly with I3, SI2 and SI1 formats. The coefficients could be modified according to the variable steps without any loss of accuracy. Therefore, this solver is more robust and more stable, but it takes more computation time than Gstiff solver. The Dstiff solver is similar to the Wstiff, but it has only one integration format I3.

The Constant-BDF solver is a stiff stable algorithm with characteristics of multi-step, variable order and fixed step. It has three integration formats I3, SI2 and SI1. This solver is very robust when using SI2 format with shorter step. Although this solver is not as fast as Gstiff and Wstiff solvers for some problems, it has high accuracy for the solution of displacement and velocity and it is not as sensitive to the discontinuity of the acceleration and force as the Gstiff solver. Therefore, the Constant-BDF solver is suitable for problems where the Gstiff fails to converge.

Trial simulations showed that the Gstiff solver failed to complete the simulation for this gearbox model. Therefore, the Constant-BDF solver with SI2 integration is adopted in this paper.

### **4. Simulation of the Ideal Gear Set**

#### **4.1 Input velocity and Output Torque**

The resistant torque acting on the output shaft of the gearbox is adopted from Table 1, i.e., the maximum output

torque of the gearbox is applied to the output shaft. The rated motor velocity from Table 1 is applied on both of the input shafts.

#### 4.2 Simulation Results of Gear Teeth Contact Force

Since the gear box drive line configuration is symmetric, the investigation is focused on the left part of the driveline. The simulation results of the gear teeth contact forces are shown from Fig.6 to Fig.8.

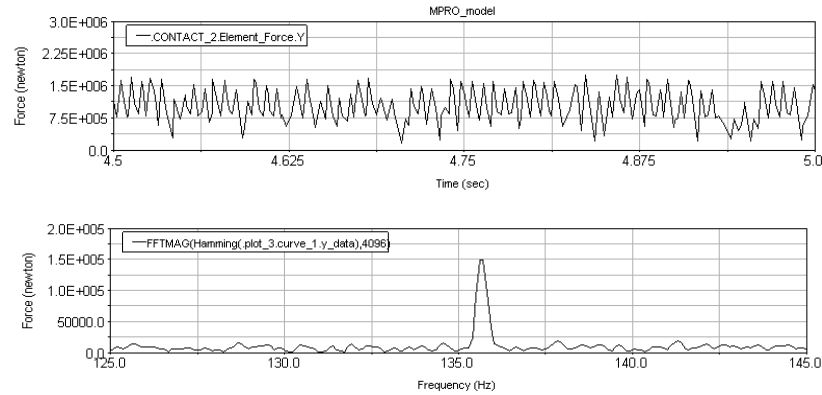


**Figure 6: First Stage Gearing Contact Forces and Frequency Spectrum**

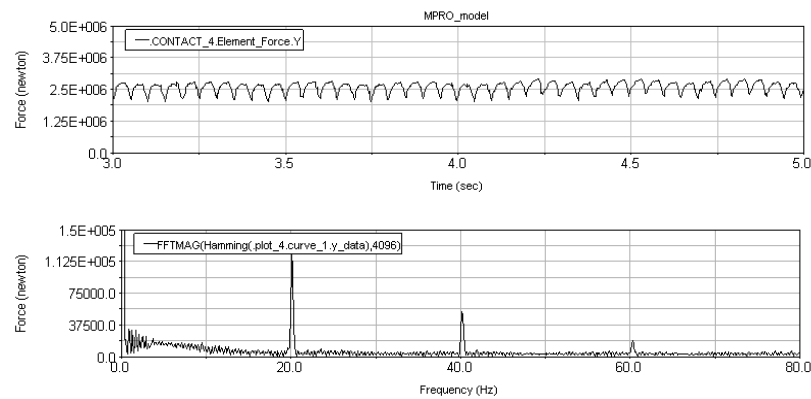


**Figure 7: Second Stage Gearing Contact Forces and Frequency Spectrum**

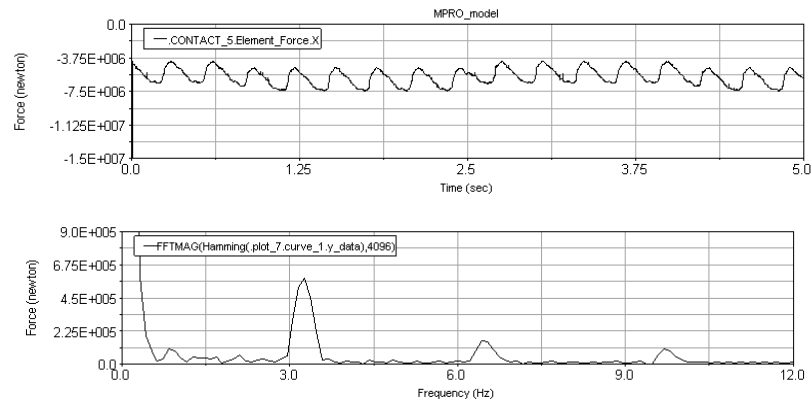


**Figure 8: Third Stage Gearing Contact Forces and Frequency Spectrum**

According to Table1 and Fig.1, the theoretical gearing frequencies from the first stage to the third stage are determined to be 135.667Hz, 20.099Hz and 3.251 Hz respectively. From frequency spectrums of Figures 6 to 8, we could conclude that the simulation results of the ideal gear set match the theoretical values well.

## 5. Gear Fault Simulation

### 5.1 Fault State of the Gearbox

Part of a tooth is removed on pinion Z5 to simulate a broken tooth state of the gearbox, as shown in Fig.9.

### 5.2 Fault Detection Based on Wavelet Decomposition

According to Table 1, the angular velocity of the pinion Z5 is 17.734 rpm, from which the impact cycle of the broken tooth pinion could be derived as 3.38s for motors driven synchronously at the rated velocity of 740 rpm. After simulation on the gearbox model with broken tooth pinion Z5, the corresponding bearing support force signal is obtained, and then it is transferred into MATLAB software.

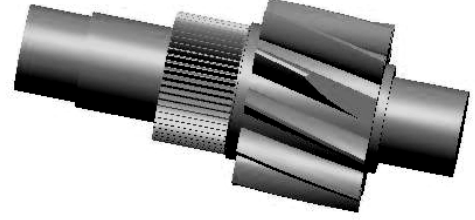


**Figure 9: Pinion Z5 with Chopped Tooth**

White noise is mixed in to simulate the real gearbox with disturbing noise. It appears at the top row marked as “S” in Fig.10. The simulation time is set for 15s, 6456 steps in ADAMS. The horizontal axis in Fig.10 represents the simulation steps and the vertical axis represents the bearing support forces (Newton). The cycling feature of the broken tooth impact is not explicit from the raw signal of the bearing support force. The Db5 wavelet with 5 levels of decomposition is used for noise canceling to make the fault feature of the broken tooth pinion distinct. The 5<sup>th</sup> level wavelet decomposition is marked as  $a_5$  in the second row of Fig.10, from which the impact cycle could be measured as 1452 steps, about 3.37s, close to the theoretical value 3.38s.

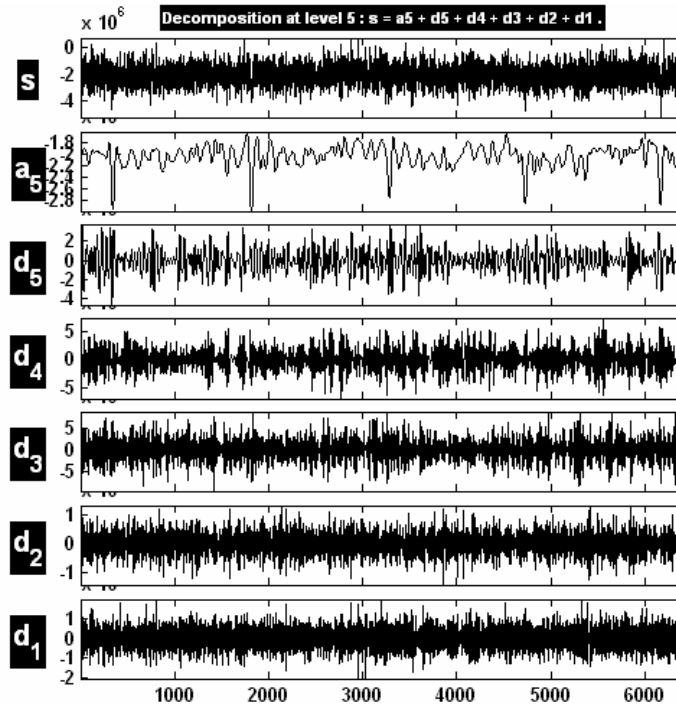


**Figure 10: Bearing Support Force Signal and Db5 Wavelet Decomposition**



## 6. Summary and Conclusion

This paper summarizes an efficient and accurate method to model gear tooth dynamics using modern engineering tools. A CAD model is transferred into multi-body dynamics software. Post processing of loading is then accomplished using the MATLAB Wavelet toolbox. The method allows for nonlinear contact mechanics to include the effects of friction, damping, and hertzian-contact in a localized region of gear mesh. The localization of the elastic portion of the model apart from the rigid body portions reduces computing time. The method is demonstrated on a large industrial gearbox model. Simulation results show that this method can predict the fault pattern of the gearbox. Wavelet analysis is shown to have good resolution in the time and frequency domain and it is effective to obtain the cyclic features of the gearbox fault signals.

## References

- [1] Wilson Q. Wang, Fathy Ismail and M. Farid Golnaraghi, Assessment of Gear Damage Monitoring Techniques Using Vibration Measurements, *Mechanical Systems and Signal Processing* (2001) 15(5), 905-922
- [2] G. Dalpiaz, A. Rivola and R. Rubini, Effectiveness and Sensitivity of Vibration Processing Techniques for Local Fault Detection in Gears, *Mechanical Systems and Signal Processing* (2000) 14(3), 387-412
- [3] A. Parey, M. El Badaoui, F. Guillet, N. Tandon, Dynamic modeling of spur gear pair and application of empirical mode decomposition-based statistical analysis for early detection of localized tooth defect, *Journal of Sound and Vibration* 294 (2006) 547–561
- [4] Saeed Ebrahimi and Peter Eberhard, Rigid-elastic modeling of meshing gear wheels in multi-body systems, *Multi-body System Dynamics* (2006) 16:55–71
- [5] Tahar Fakhfakh, Fakher Chaari and Mohamed Haddar, Numerical and experimental analysis of a gear system with teeth defects, *Int J Adv Manuf Technol* (2005) 25: 542–550
- [6] I. Ciglaric and A. Kidric, Computer-aided derivation of the optimal mathematical models to study gear-pair dynamic by using genetic programming, *Struct Multidisc Optim* (2006) 32: 153–160
- [7] M. Pimsarn and K. Kazerounian, Pseudo-interference stiffness estimation, a highly efficient numerical method for force evaluation in contact problems, *Engineering with Computers* (2003) 19: 85–91
- [8] BI Feng-rong, Cui Xin-tao, Liu Ning, Computer Simulation for Dynamic Meshing Force of Involute Gears, *Journal of Tianjin University*, Vol.38No.11,Nov.2005
- [9] Sejoong Oh, Karl Grosh, James R. Barber, Energy Conserving Equations of Motion for Gear Systems, *Transactions of the ASME*, Vol. 127, APRIL 2005
- [10] K. L. Johnson, *Contact Mechanics*, Cambridge University Press, 1985
- [11] Monsak Pimsarn a, Kazem Kazerounian, Efficient evaluation of spur gear tooth mesh load using pseudo-interference stiffness estimation method, *Mechanism and Machine Theory* 37 (2002) 769–786
- [12] MSC Inc., MSC ADAMS reference manual